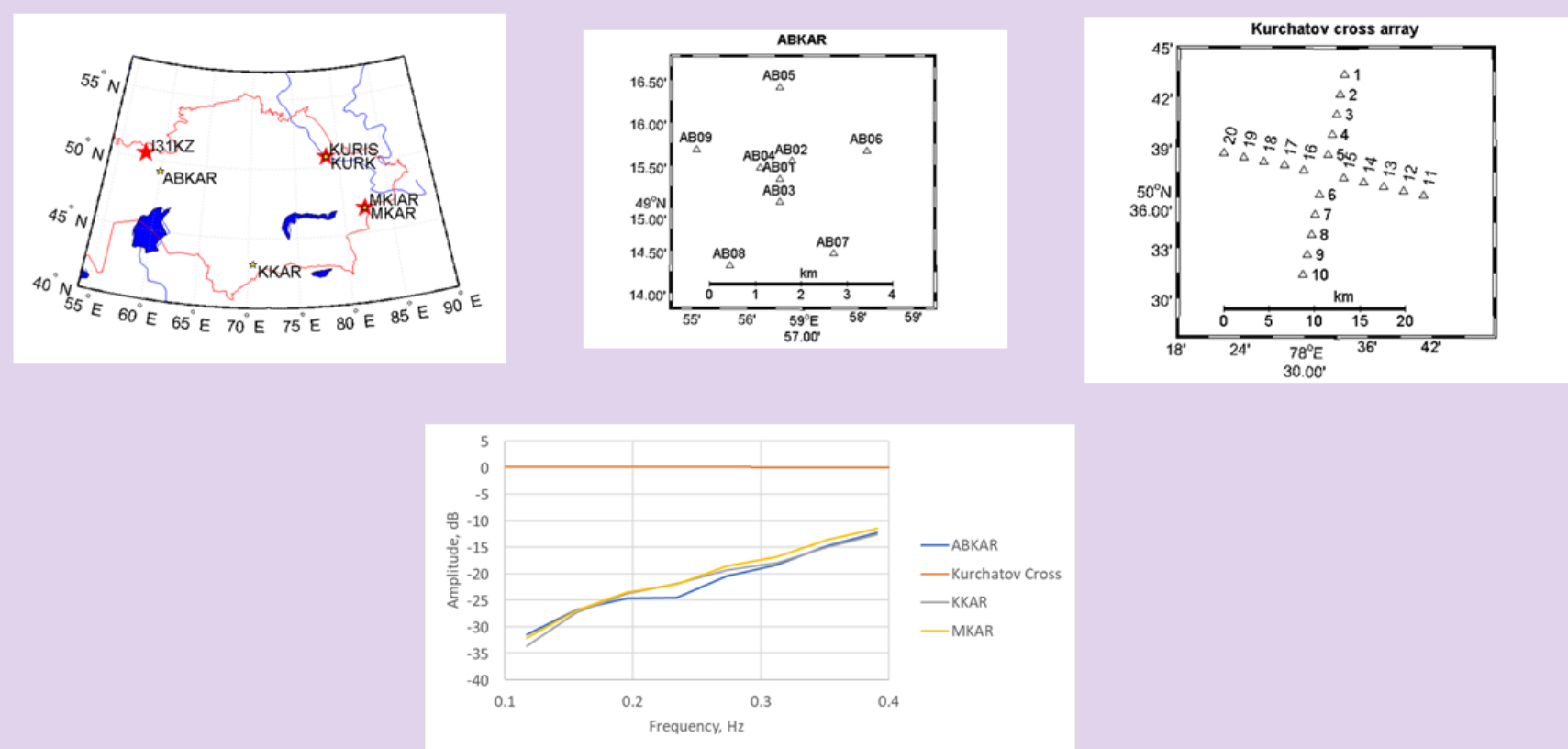


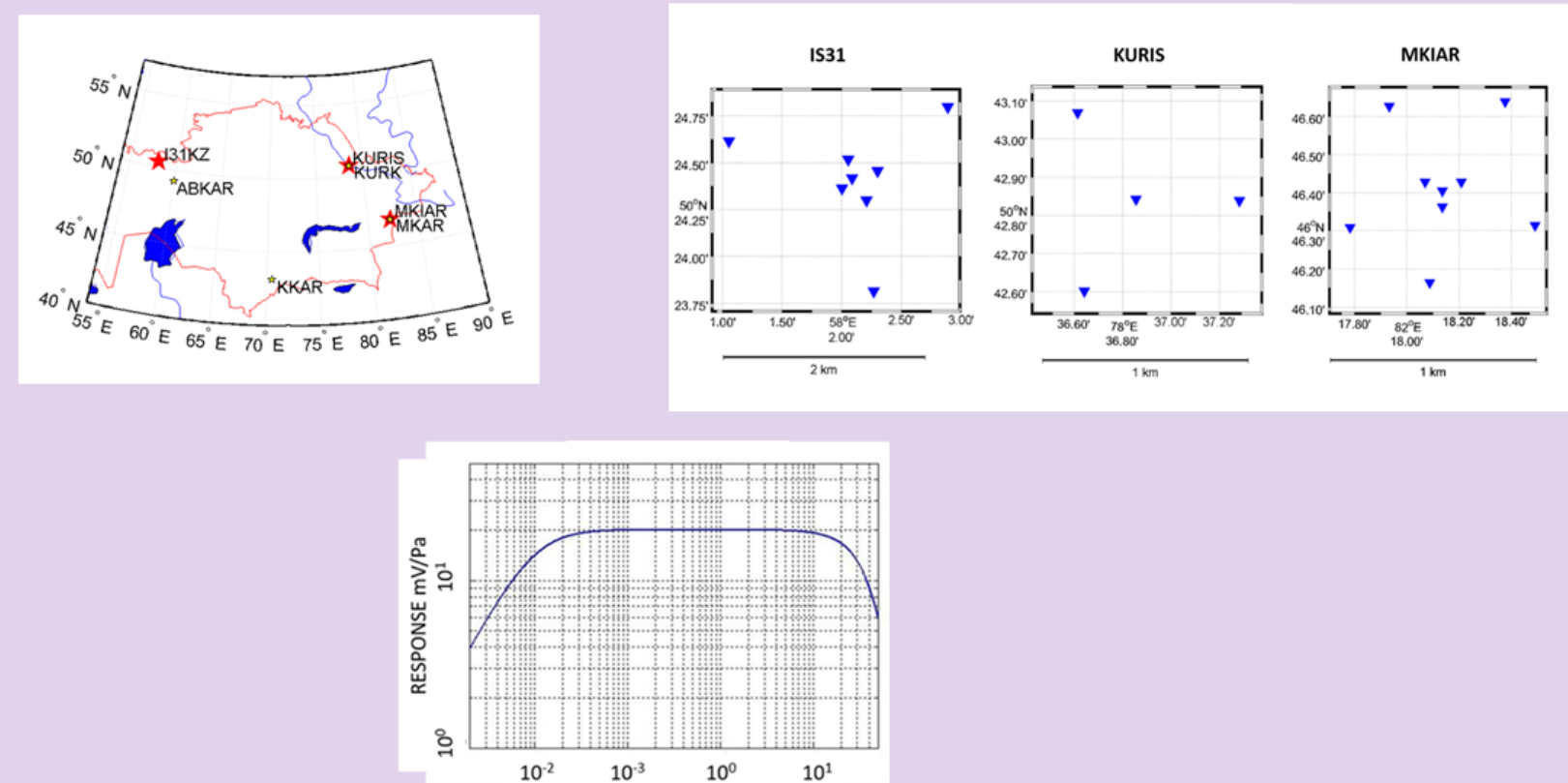
ABSTRACT

The monitoring network of the Kazakhstani Institute of Geophysical Researches includes seismic and infrasound arrays. The PMCC method helps identifying microseisms in seismic records and microbaroms in infrasound records effectively. Simulation of the microbarom strength, propagation path and signal attenuation are well developed for the moment, and for microseisms as well. However, the bathymetry effect on the source intensity shall be taken into account to model microseisms. Results of the source parameter simulations and microbaroms and microseisms detections are compared at 7 Kazakhstani seismic and infrasound arrays. These comparisons are also carried out between collocated seismic and infrasound arrays. Similarities and differences between the reconstructed source regions of microseisms and microbaroms are discussed. Beside this study, the advantages of integrating the infrasound and seismic methods have been shown for studying seismoacoustic signals from severe storms.

OBSERVATION NETWORK: SEISMIC ARRAYS



OBSERVATION NETWORK: INFRASOUND ARRAYS

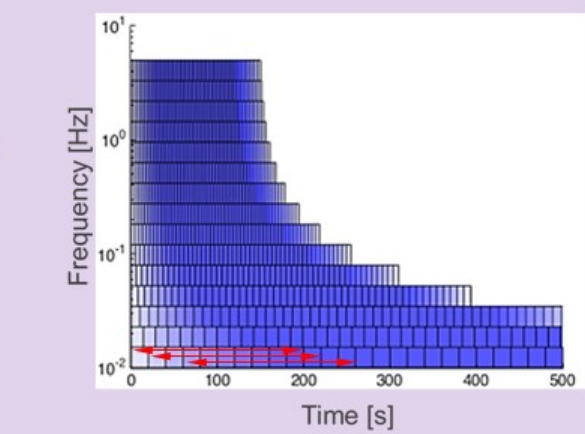
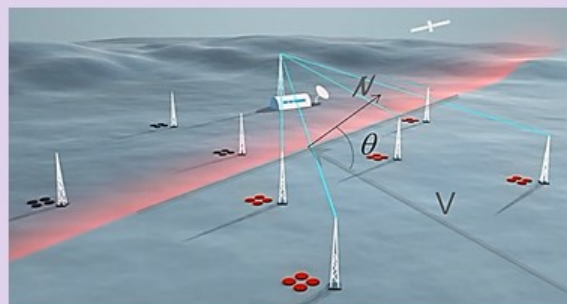


THE PMCC METHOD

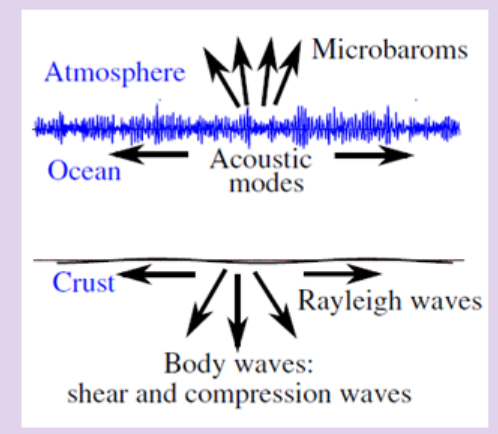
PMCC = Progressive MultiChannel Correlation (Cansl, 1995)

Time-domain correlation method

- filtered signals (narrow bands)
- compute cross-correlation $C_{ij}(\tau)$ between filtered records of stations S_i and S_j
- time delay: $\tau_{ij} = \arg \max_{\tau} |C_{ij}(\tau)|$
- detection criteria: $\phi_i = \text{Phase}[\sum_j S_j(f)] = 2\pi f \tau_i$, $\phi_i(f) + \phi_j(f) + \phi_k(f) = 0$
- least-squared solution (2D): $S = (A^T A)^{-1} A^T \Delta T$, $V = \sqrt{S^T \cdot S^T}$, $\theta = \arctan(\frac{S_y}{S_x})$
- a real-time process operational at CITATO

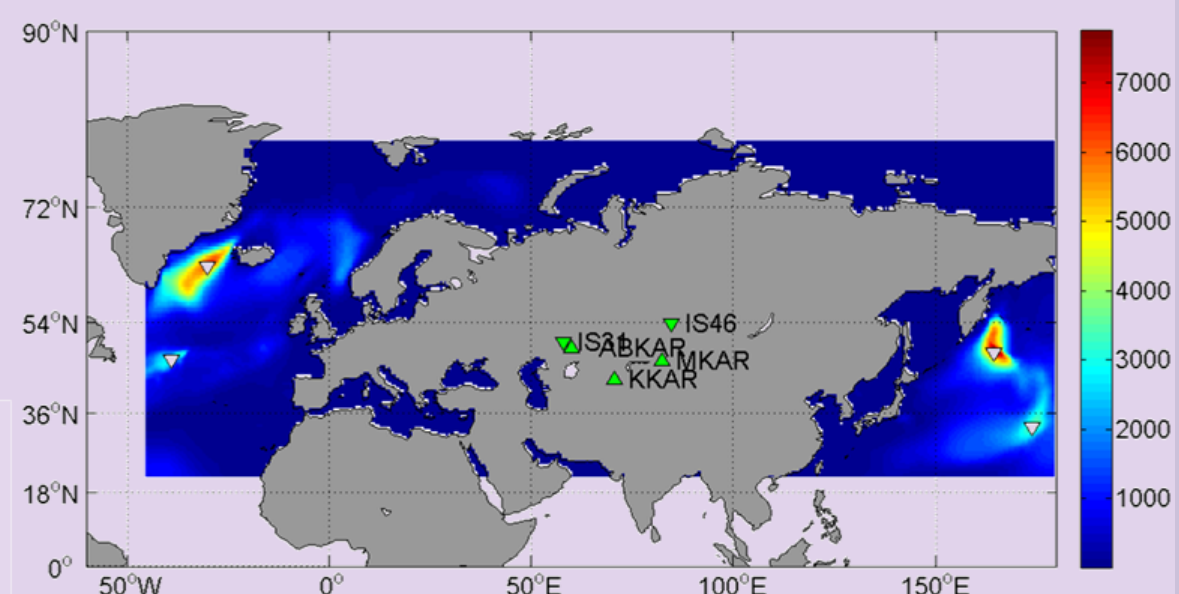


SOURCE MODELLING: EXAMPLE OF A SOURCE MODEL (ARDHUIN ET AL. 2011)



(From Ardhuin and Herbers, 2013)

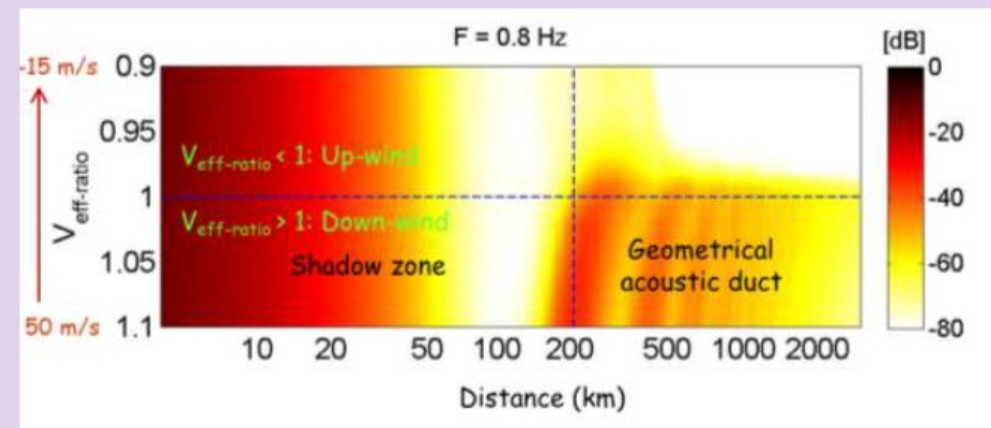
- Source strength given by non-linear interaction of counter propagating waves (Longuet-Higgins, 1950; Hasselmann, 1963; Waxler and Guilbert, 2006; Ardhuin and Herbers, 2013)
- Operational microseism source model distributed by Ifremer (<http://ftp.ifremer.fr/ifremer/ww3d/>) (Ardhuin et al., 2011)



Local maxima are found in accordance with https://de.mathworks.com/matlabcentral/mc-downloads/downloads/submissions/37388/versions/13/previews/FastPeakFind.m/index.html?access_key=

MICROBAROM ATTENUATION

ATTENUATION RELATION (LE PICHON 2011)



- At large distance, downwind, the attenuation weakly depends on wind conditions
- A "binary"-like pattern

$$P_{\text{receiver}} / P_{\text{source}} = R^{-1} \cdot 10^{(aR)/20} + R^0 / (1 + 10^{(aR)/20})$$

- $a(f)$: air losses of direct waves (e.g., Beranek 1954)
- $b(V_{\text{eff-refr}}, f)$: geometrical spreading of ducted waves
- $\delta(\text{cst})$: width of shadow zone (ranges between 120 and 250 km)
- $\sigma(f)$: std deviation of shadow zone's width

MICROSEISM ATTENUATION

ATTENUATION RELATION (STUTZMANN 2012)

The ocean is discretized on a grid and each source S_i located at the colatitude-longitude grid point (ϕ, λ) generates Rayleigh waves which propagate along the Earth surface to the station at the group velocity $U(f_i)$. For a given station located at colatitude ϕ and longitude λ , the power spectrum of the vertical ground displacement is the sum over all grid points to consider the contribution of all sources. Taking into account the geometrical spreading and the seismic attenuation $Q(f_i)$, the power spectral density of the vertical displacement is

$$F_{\delta}(\lambda, \phi, f_s) = \int_0^{2\pi} \int_0^{\pi} \frac{S_{DF}(f_s)}{a \sin(\alpha)} P(f_s) \exp\left(-\frac{2\pi f_s a \alpha}{QU}\right) a^2 \sin(\phi') d\lambda' d\phi'$$

where a is the earth radius, α is the angular epicentral distance and $a^2 \sin(\phi) d\lambda d\phi$ is the elementary surface area. To empirically take into account the 3-D propagation or local effects on the spectrum amplitude, a dimensionless parameter $P(f_i)$ is introduced.

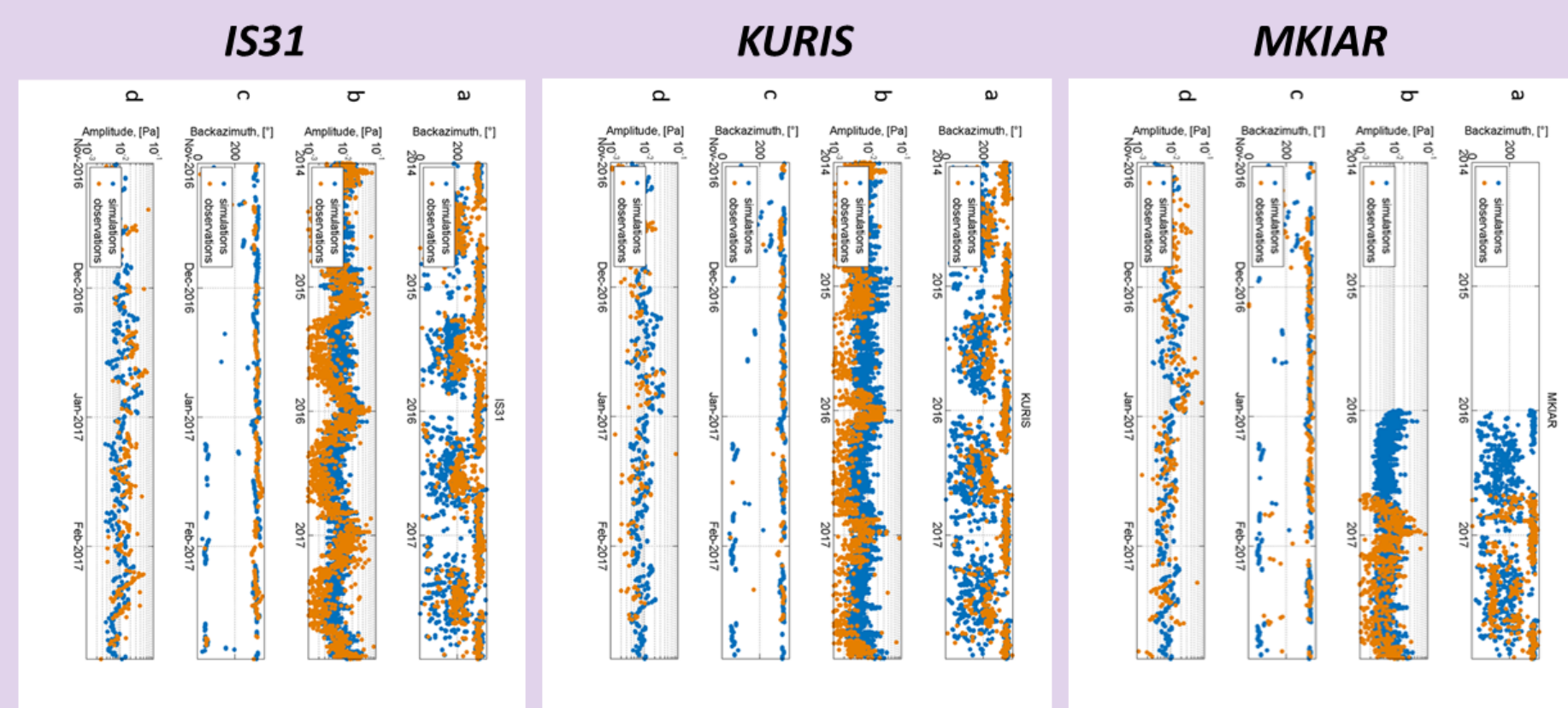
BATHYMETRY EFFECT ON THE MICROSEISM SOURCE INTENSITY

Longuet-Higgins (1950) showed that the pressure fluctuations are not attenuated with depth but transmitted to the ocean bottom as acoustic waves. Depending on the ratio between the wavelength of the acoustic waves and the ocean depth, resonance effects can occur leading to a modulation of the pressure fluctuations at the ocean bottom. Then, the corresponding seismic source power spectral density at the ocean bottom is

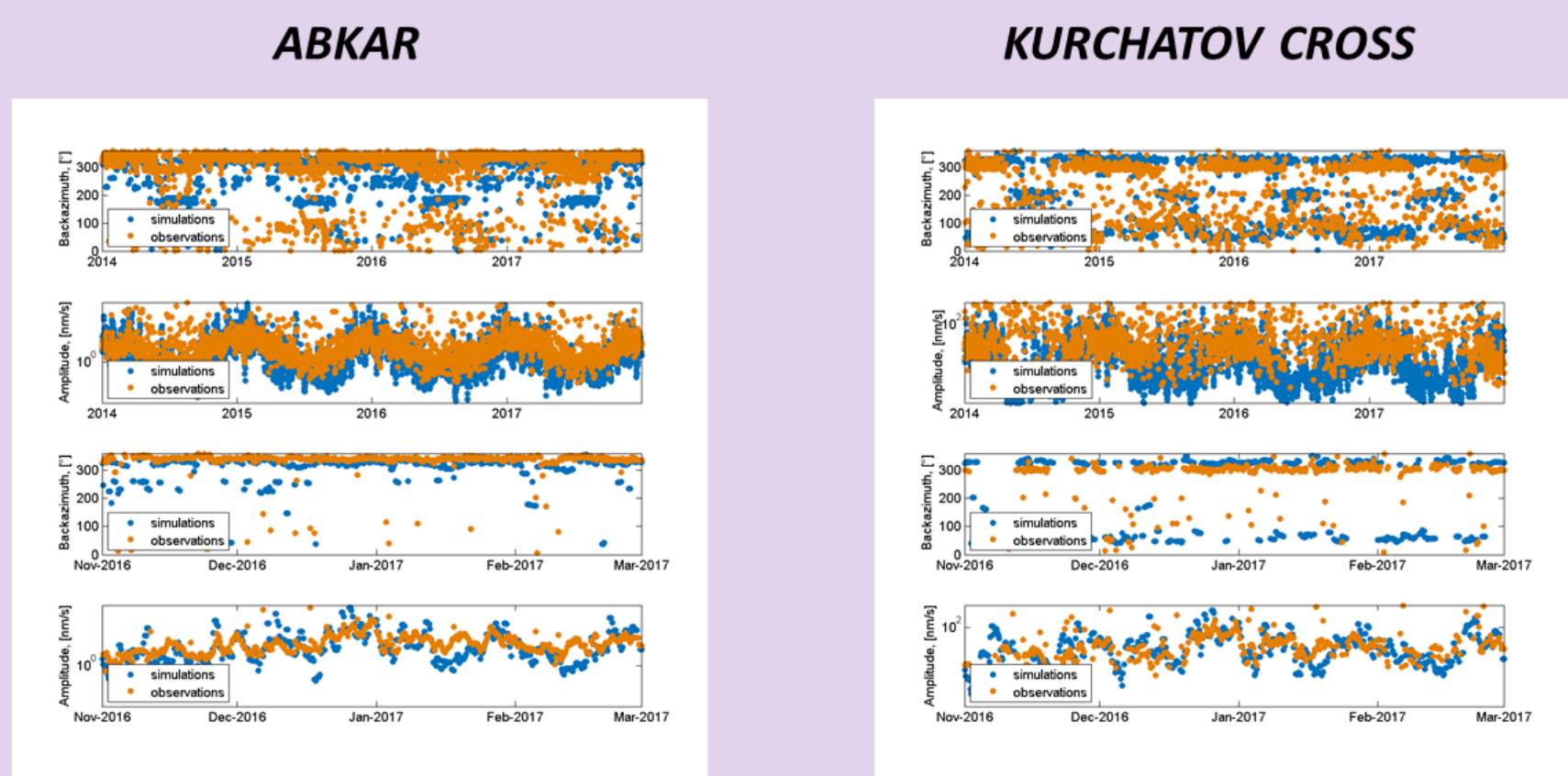
$$S_{DF}(f_s = f_2) = \frac{2\pi f_s}{\rho_s^2 \beta^2} \left[\sum_{m=1}^N c_m^2 \right] F_p(\mathbf{K} \simeq 0, f_2 = 2f)$$

S_{DF} is in mHz^{-1} , ρ_s and β are respectively the density and S -wave velocity in the crust. f_s is the seismic frequency which is equal to the pressure fluctuation frequency f_p and it is the double of the ocean wave frequency f . Coefficients c_m correspond to the compressible ocean amplification factor (from Stutzmann et al, 2012).

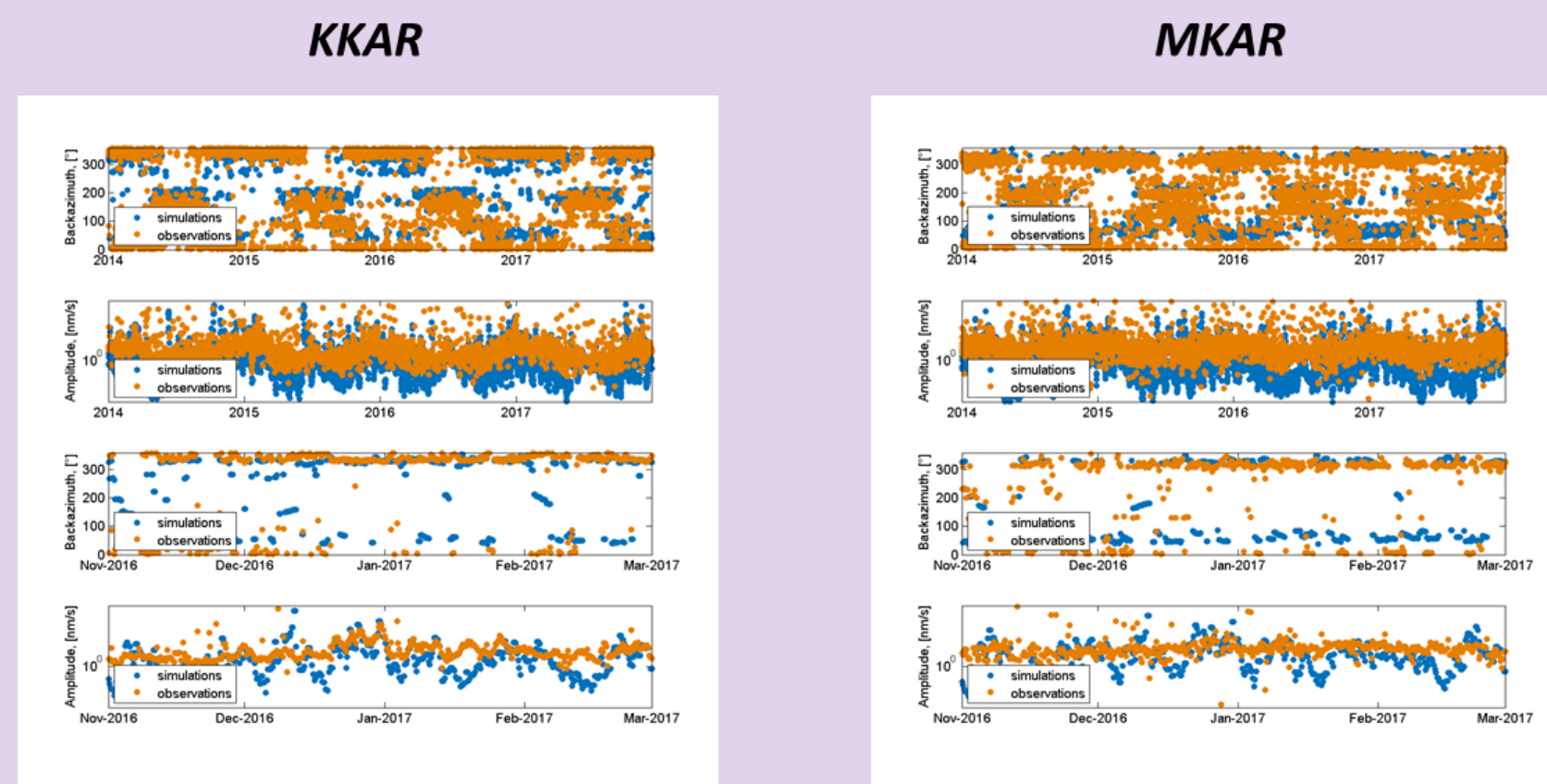
COMPARISON OF THE MICROBAROMS DETECTIONS AND OBSERVATIONS



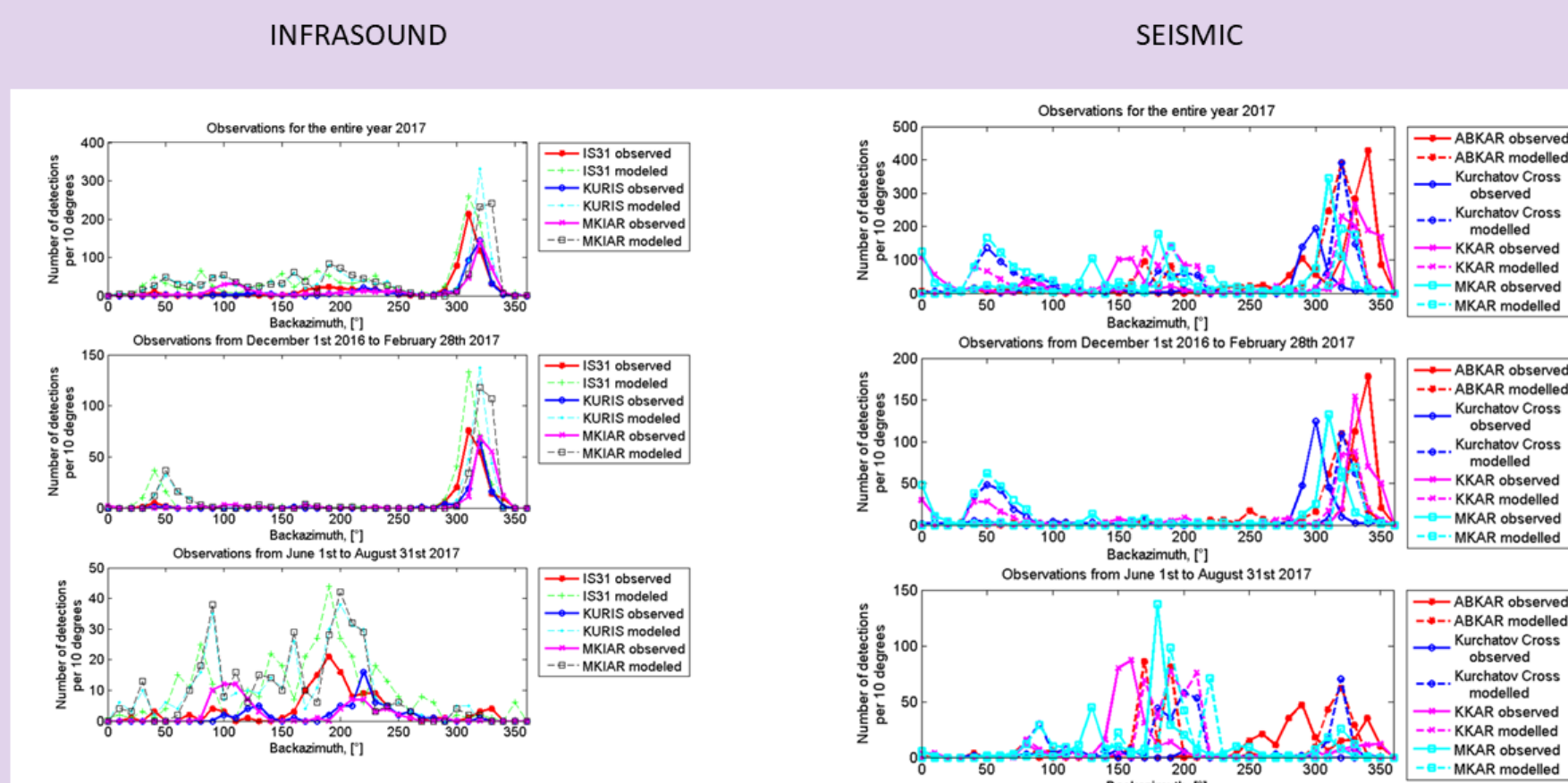
COMPARISON OF THE MICROSEISMS DETECTIONS AND OBSERVATIONS I



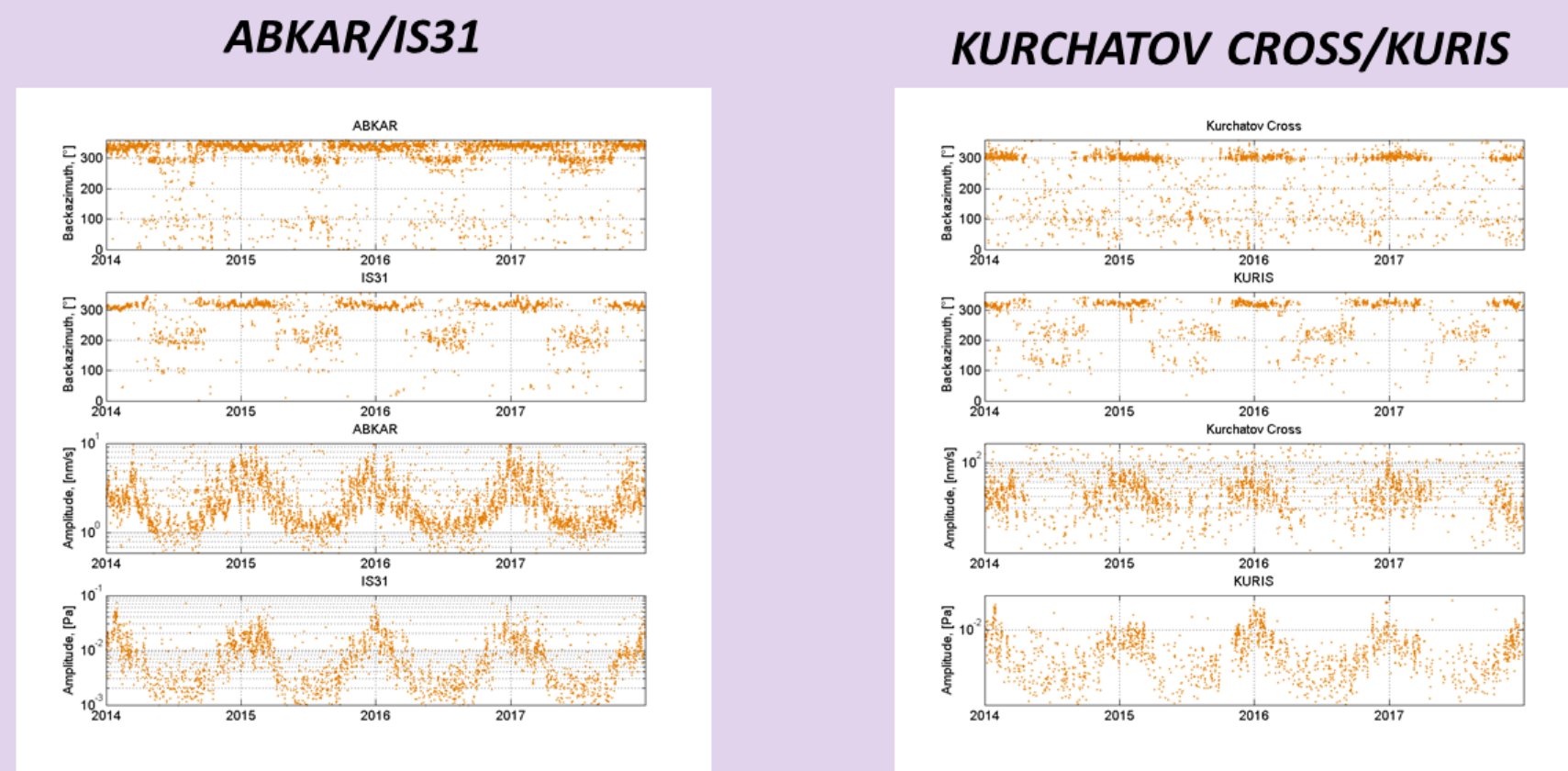
COMPARISON OF THE MICROSEISMS DETECTIONS AND OBSERVATIONS II



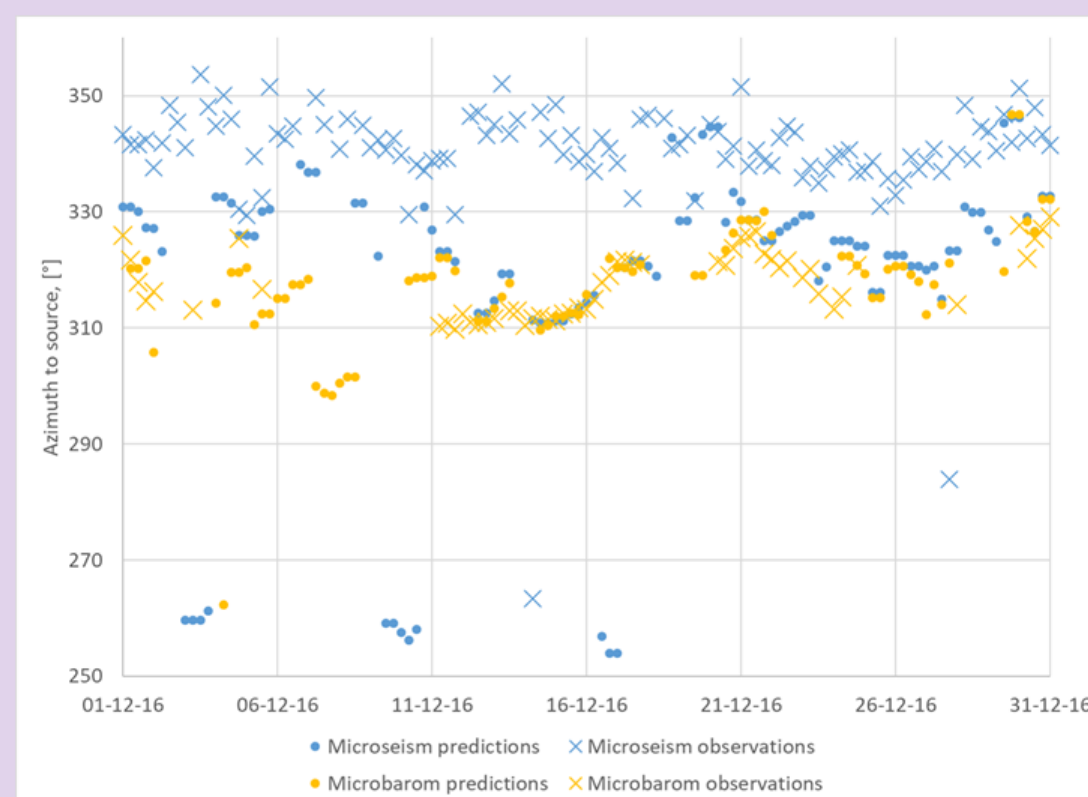
MAIN SOURCE REGIONS VS. SEASON



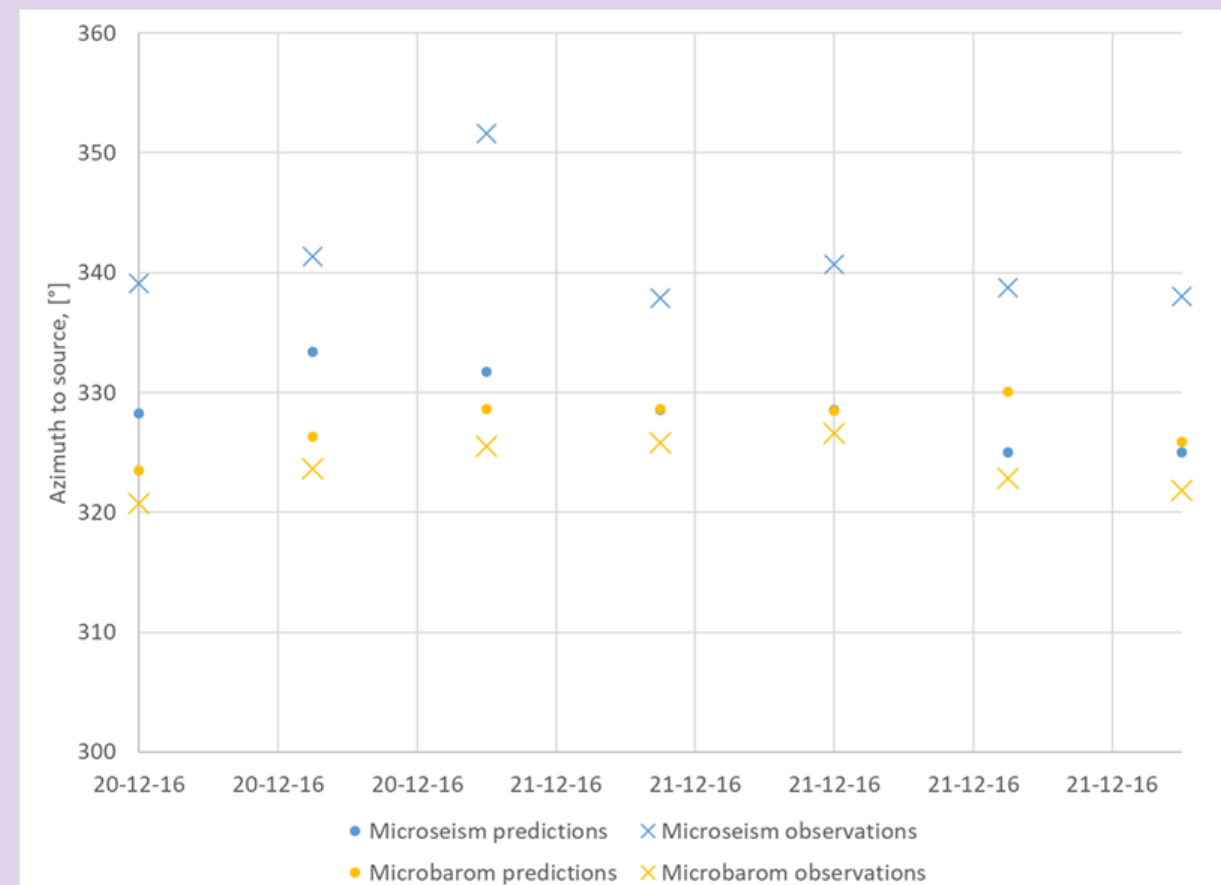
COMPARISON OF THE MICROSEISMS AND MICROBAROM DETECTIONS



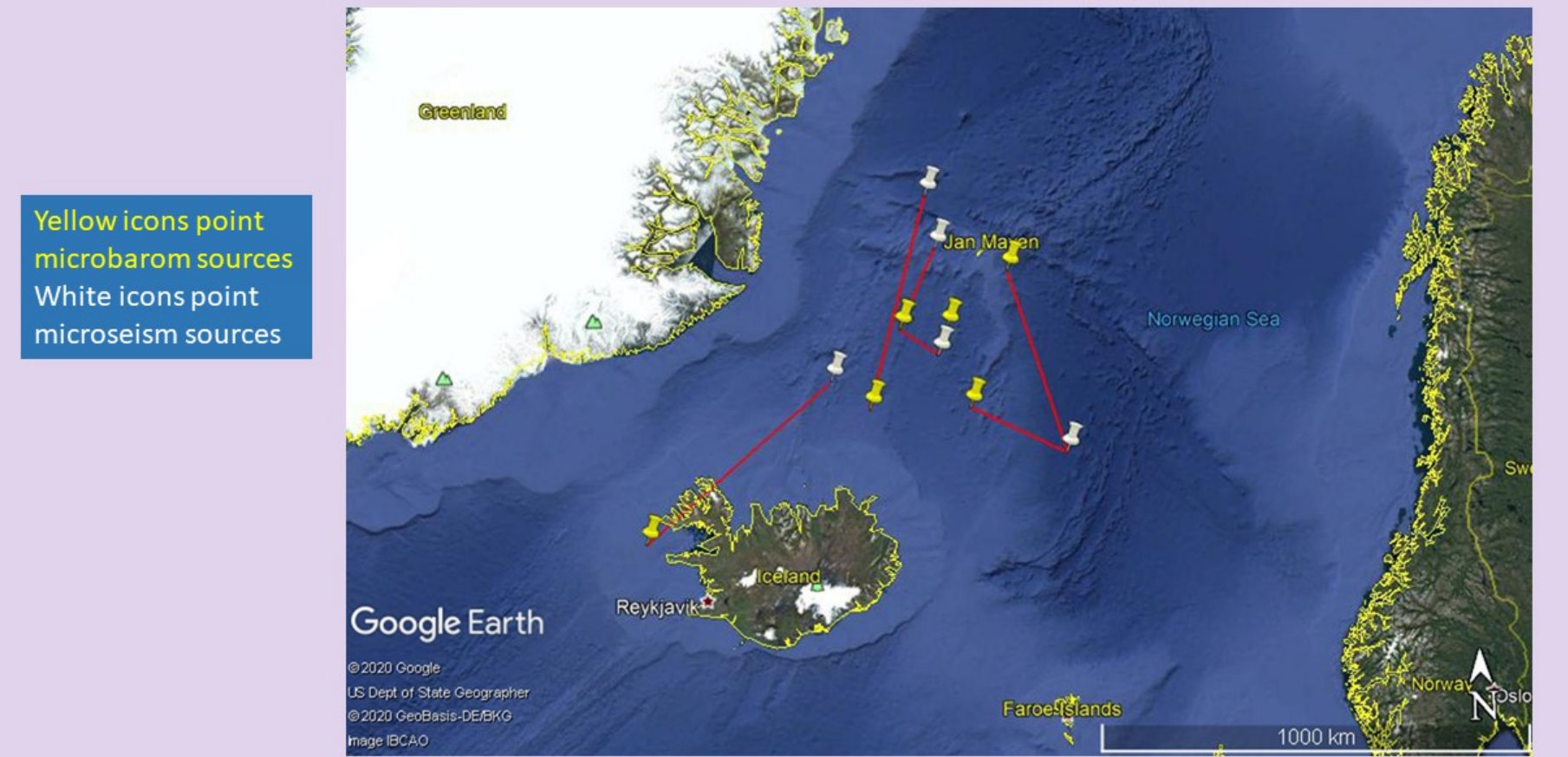
COMPARISON OF THE MICROSEISMS AND MICROBAROM DETECTIONS/PREDICTIONS: ONE MONTH OF DATA



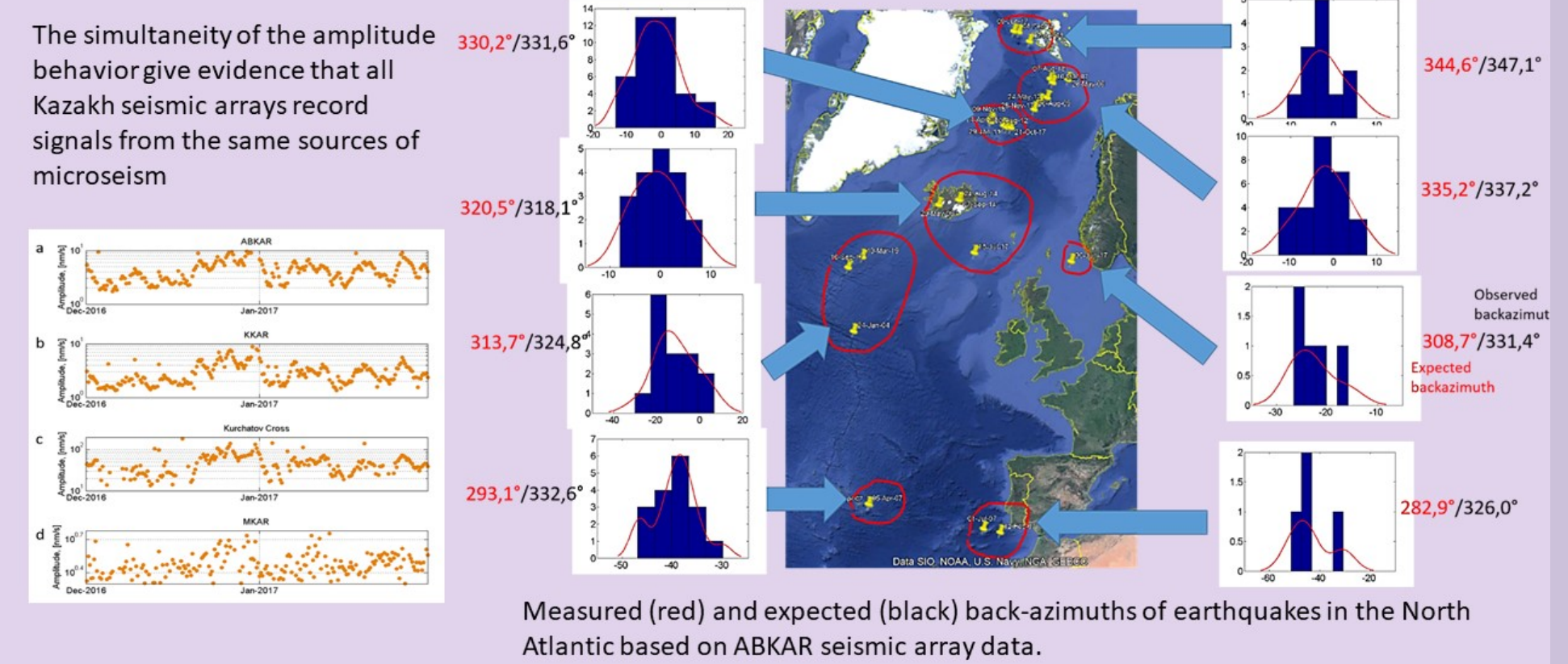
COMPARISON OF THE MICROSEISMS AND MICROBAROM DETECTIONS/PREDICTIONS: DETAILING



COMPARISON OF THE MICROSEISMS AND MICROBAROM SOURCE REGIONS



DISCUSSIONS: WHAT IS THE REASON FOR THE MICROBAROM OBSERVATIONS/PREDICTIONS MISMATCH?



Conclusion 1: winter

In winter, the most intense oceanic microbarom and microseism sources reside in the northern hemisphere, and their signals prevail on infrasonic and seismic records in the 0.1 - 0.4 Hz frequency band. Amplitudes of these signals are higher significantly than amplitudes of all other permanent sources. Source Regions of the microbaroms and microseisms don't coincide due to the bathymetry effect. But this difference is not dramatic for the distant Kazakhstani observation network. This allows to study signal sources using a fusion of infrasonic and seismic approaches. This fusion is mutually beneficial in the following aspects:

- Azimuthal error due to array geometry at seismic arrays is ~ 10 times higher than at infrasonic stations due to shorter wavelength;
- Detectability of the infrasonic arrays is much lower than that of seismic ones as propagation medium of infrasonic is unstable;
- The recording of microbaroms is unstable, inter alia, due to dramatic noise level changes while The level of seismic noise at seismic arrays is stable and low.
- Infrasonic arrays register virtually one type of wave for signals from North Atlantic. In contrast, seismic energy comes to Kazakhstan following various paths, the recorded signal is a sum of a number of different phases;
- seismic arrays shown significant statistical azimuth corrections (Smirnov et al., 2011), associated with a non-uniform medium at array locations while infrasonic stations have practically no error.

But!!! Additional studies are required to confirm whether source-specific station correction is the reason of the microseism detection/prediction mismatch.

Conclusion 2: summer

In summer, most powerful microbarom and microseism sources are in the southern hemisphere. Detections of the signals from the sources being southward from the Kazakh network do not dominate amongst the detections of the Kazakh network at this period. Apparently, amplitudes of the oceanic microbaroms and microseisms in Kazakhstan are getting equal or even less than the amplitudes of signals from sources of another nature. This fact makes difficult a possibility to studying the signals from oceanic storms in the southern hemisphere. Therefore, using of the data of seismo-acoustic network in the southern hemisphere would be more efficient for detailing global natural noise sources in this area.

